PHYSICAL REVIEW B **89**, 100104(R) (2014)

Unique single-domain state in a polycrystalline ferroelectric ceramic

Hanzheng Guo,[1] Chao Zhou,[2] Xiaobing Ren,[2] and Xiaoli Tan[1,*]

[1]*Department of Materials Science and Engineering, Iowa State University, Ames, Iowa 50011, USA*

[2]*Multi-disciplinary Materials Research Center, Frontier Institute of Science and Technology, Xi'an Jiaotong University, Xi'an 710049, China*

(Received 12 January 2014; revised manuscript received 4 March 2014; published 17 March 2014)

Non-180° ferroelectric domains are also ferroelastic domains; their existence in polycrystalline materials is to relieve internal stresses generated during solid-solid phase transitions and minimize the elastic distortion energy. Therefore, grains with random orientations in polycrystalline ceramics are always occupied by many domains, especially in the regions close to grain boundaries. In this Rapid Communication, we report the observation of a single-domain state in a $BaTiO_3$-based polycrystalline ceramic at intermediate poling electric fields with *in situ* transmission electron microscopy. The grains in the virgin ceramic and under high poling fields are found multidomained. The unique single-domain state is believed to be responsible for the ultrahigh piezoelectric property observed in this lead-free composition and is suggested to be of orthorhombic symmetry for its exceptionally low elastic modulus.

DOI: 10.1103/PhysRevB.89.100104 PACS number(s): 77.80.Dj, 68.37.Lp, 77.65.−j, 77.84.Cg

Domains are formed in ferroelectric crystals to minimize the electrostatic energy associated with the spontaneous polarization and the elastic energy due to lattice distortion at the displacive solid-solid phase transitions [1–7]. The electrostatic energy is minimized when the polarization vectors of adjacent domains are adopted such that div $\boldsymbol{P} = 0$ at the domain walls [3]. For non-180° ferroelectric domains, this condition is satisfied with the "head-to-tail" arrangement of polarization vectors across the domain wall. For 180° domains, the electrostatic energy drives the domain wall parallel to the polarization vectors [3]. Non-180° ferroelectric domains are also ferroelastic domains due to the orientation difference of the spontaneous strain tensors across the domain wall [2,3]. They are created primarily during the paraelectric to ferroelectric phase transition to minimize the elastic energy through releasing the internal stresses [1]. Further ferroelectric to ferroelectric phase transitions at lower temperatures also contribute to the formation of non-180° domains.

In ferroelectric single crystals, the multidomain state is still favored for its low electrostatic energy even though no mechanical constraints are present on the crystal surfaces [1–3]. A single-domain state could presumably be achieved by electrical poling through electric-field-induced domain switching [2,3]. However, elimination of domain walls in single crystals with electric field is not always guaranteed [8,9]. In a polycrystalline ceramic, each grain is mechanically confined by its neighboring grains, which usually leads to a complex multidomain structure as the favored states of low energy [1]. A single-domain state of the grains is hence extremely difficult, if not impossible, to be reached by poling because of high internal stresses from the incompatible transformation strain at grain boundaries and nonuniform electric fields from the anisotropy in dielectric permittivity [2]. With either *ex situ* or *in situ* observations, previous experimental studies invariably indicate the existence of multiple domains in grains of polycrystalline ceramics, including poled $BaTiO_3$ with large grain sizes [10], poled $(K_{0.5}Na_{0.5})NbO_3$ ceramics [11], poled $Pb(Zr,Ti)O_3$ ceramics [12], as well as $(Bi_{1/2}Na_{1/2})TiO_3$–$BaTiO_3$ ceramics under applied fields during electrical poling [13]. Here, we report the observation of poling-induced single-domained grains in the polycrystalline ceramic of $0.5Ba(Zr_{0.2}Ti_{0.8})O_3$–$0.5(Ba_{0.7}Ca_{0.3})TiO_3$, a lead-free composition showing ultrahigh piezoelectric coefficients [14].

The ceramic was prepared using the solid-state reaction method with details reported previously [15]. The average grain size was determined to be 13.1 μm. For the electric field *in situ* transmission electron microscopy (TEM) experiments [13,16–19] disk specimens (3 mm in diameter) were prepared from as-sintered pellets through standard procedures including grinding, cutting, dimpling, and ion milling. Prior to ion milling, the dimpled disks were annealed at 200°C for 2 h. *In situ* TEM experiments were carried out on a Phillips CM-30 microscope operated at 200 kV.

The evolution of the ferroelectric domains in the ceramic during electrical poling is exemplified with a grain imaged along its [112] zone axis, as shown in Fig. 1. In the virgin state [Fig. 1(a)], two sets of long lamellar domains are observed. In the upper left part of Fig. 1(a), the previously reported hierarchical domain structure [20] is also seen with nanodomains being developed within the wedge-shaped domains. At the nominal poling field of 1.00 kV/cm, significant changes in the domain morphology are observed, indicating extensive domain switching activities at this low level of electric field [Fig. 1(b)]. It should be noted that the multidomain state is still preserved. When the electric field reaches a nominal value of 1.33 kV/cm, all of the domain walls disappear; the whole grain unexpectedly becomes a large single domain, as shown in Fig. 1(c). This single-domain state is found not stable against higher poling electric fields. At the field of 4.50 kV/cm, one set of long lamellar domains are formed [Fig. 1(d)]. The corresponding electron diffraction patterns during the poling process are also displayed in Fig. 1. Neither detectable changes in the diffraction pattern nor the appearance of superlattice spots are observed.

It should be emphasized that the grain shown in Fig. 1 is surrounded by neighboring grains. The observation of a grain with no domain walls in a dense polycrystalline ceramic is highly unusual because of the mechanical confinement imposed by neighboring grains. To the authors' knowledge,

*Corresponding author: xtan@iastate.edu

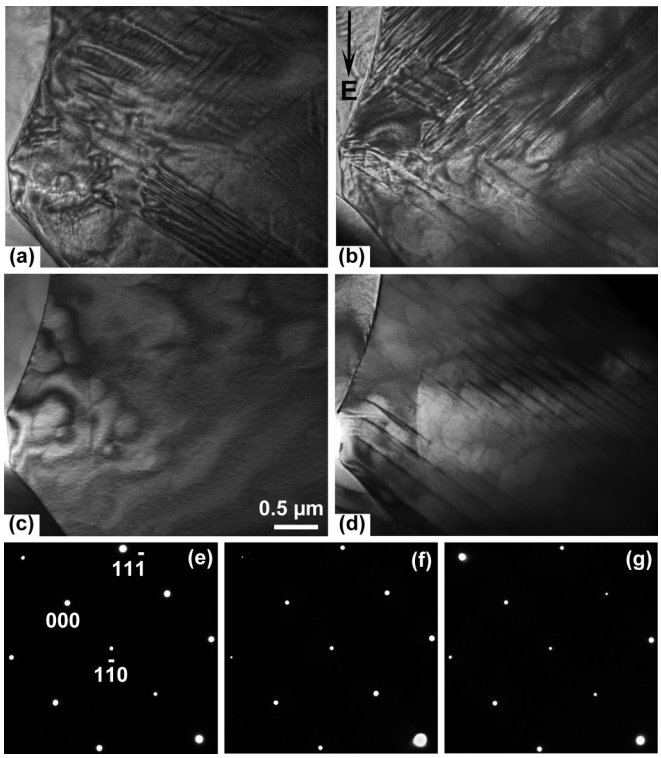

FIG. 1. *In situ* TEM observations of a grain along the [112] zone axis in the $0.5Ba(Zr_{0.2}Ti_{0.8})O_3$–$0.5(Ba_{0.7}Ca_{0.3})TiO_3$ ceramic under electric fields. Bright-field micrographs at (a) virgin state, (b) 1.00 kV/cm, (c) 1.33 kV/cm, and (d) 4.50 kV/cm are displayed. The direction of poling field is indicated by the dark arrow in (b). Representative selected area diffraction patterns are recorded at (e) virgin state, (f) 1.33 kV/cm, and (g) 4.50 kV/cm.

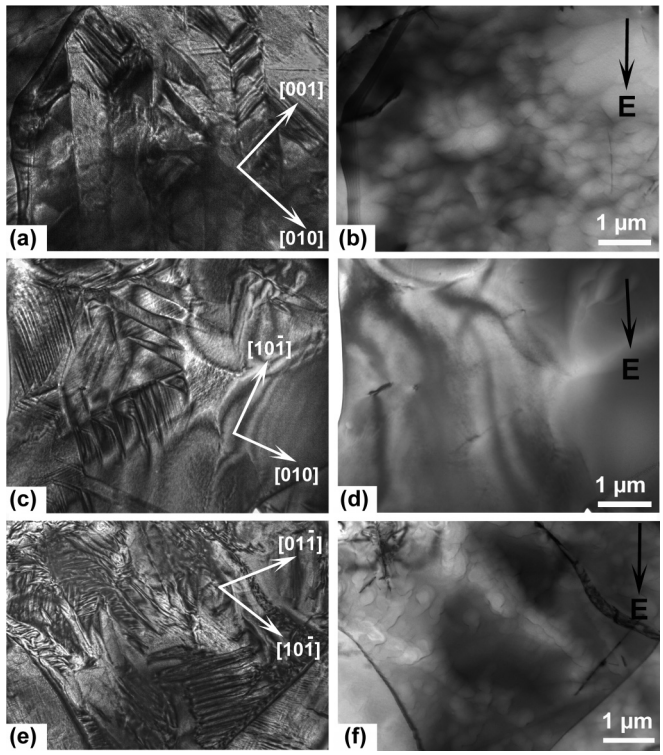

FIG. 2. *In situ* TEM observations of a series of grains in the same specimen of the $0.5Ba(Zr_{0.2}Ti_{0.8})O_3$–$0.5(Ba_{0.7}Ca_{0.3})TiO_3$ ceramic. Bright-field micrographs are displayed for a grain along (a) the [100] zone axis in the virgin state, (b) the [100] zone axis at 1.33 kV/cm, (c) the [101] zone axis in the virgin state, (d) the [101] zone axis at 2.50 kV/cm, (e) the [111] zone axis in the virgin state, and (f) the [111] zone axis at 3.20 kV/cm. The micrographs in (b), (d), (f) were recorded within 1 min after the applied field reached the specified values. Two essential crystallographic directions in each zone axis are shown by bright arrows in (a), (c), and (e). The direction of the poling field is indicated by the dark arrow in (b), (d), and (f).

the electric-field-induced transition from a multidomain to a single-domain state has only been experimentally observed in single crystals [9,21,22].

To make sure this single-domain state can be reproduced in different grains in the ceramic, a number of grains (>30) in several TEM specimens were analyzed. The presence of the single-domain state at low poling fields was repeatedly observed in all the examined grains with varied grain sizes. Figure 2 shows the results on three representative grains in the same TEM specimen with their zone axis along [100], [101], and [111], respectively. In the virgin state of the ceramic [Figs. 2(a), 2(c), and 2(e)], multiple domains with complicated hierarchical structures are observed for all three grains. This hierarchy feature is more apparent in the upper middle part of the [101]-aligned grain [Fig. 2(c)], where very fine domains with sizes of 100 ∼ 300 nm are observed within the [010]-oriented wedge-shaped large domains. The domain walls in the virgin state are most likely on the {001} and {110} crystallographic planes. During poling at very moderate field values, the multidomain to single-domain transition is clearly observed to occur at different nominal applied fields: 1.33 kV/cm for the [100]-, 2.50 kV/cm for the [101]-, and 3.20 kV/cm for the [111]-aligned grains, respectively. Again, there is no apparent change in the corresponding electron diffraction patterns. It is noticed that the single-domain state starts to appear at different poling fields in different grains. This could be a result of the following facts: (1) The electric field in the TEM specimen is not uniform due to the presence of a central perforation. The actual field may be distorted, intensified, or diluted by the perforation [17]. Since the exact value of the actual field is not known, the values reported here are the nominal ones (the applied voltage divided by the electrode spacing). (2) The grains in the ceramic are typically in a size above 10 μm [23]. An orientation dependence of the poling response is expected, as in single crystals of other ferroelectric perovskites [24].

It is noticed that two other states, a nanodomains state [25,26] and an isotropization state [27–29] have similar appearances in TEM bright field imaging as those shown in Fig. 1(c), and Figs. 2(b), 2(d), and 2(f). However, electric field is known to favor large ferroelectric domains with long-range polar ordering over nanodomains with short-range ordering, as demonstrated previously in $(Bi_{1/2}Na_{1/2})TiO_3$–$BaTiO_3$ solid solutions [13,18] and $Pb(Mg_{1/3}Nb_{2/3})O_3$-based ceramics [30]. The possibility of a nonpolar isotropic phase can also be ruled out as it usually appears as a transient phase during temperature-induced transition [29]. An electric field, as a driving force for phase transition with a

polar cylindrical symmetry of ∞m [31], is not expected to favor the isotropization state [32]. Most importantly, our piezoelectric coefficient d_{33} measurements on bulk samples indicate a fast increase to ~200 pC/N at poling fields around 3.50 kV/cm. The formation of a nonpolar isotropic phase will diminish the piezoelectricity. Therefore, we argue that the $0.5Ba(Zr_{0.2}Ti_{0.8})O_3$–$0.5(Ba_{0.7}Ca_{0.3})TiO_3$ ceramic is in a unique single-domain state with long-range ferroelectric ordering formed under very moderate poling fields.

Non-180° domains are needed in grains in a polycrystalline ferroelectric ceramic to accommodate internal stresses and are known to persist in regions adjacent to grain boundaries even at very high poling fields [33]. Therefore, the single-domain state observed in this study seems to indicate low internal stresses in the ceramic, which we suggest could be achieved through an electric-field-induced transition to a pure orthorhombic phase. Previous symmetry analysis reveals that the $0.5Ba(Zr_{0.2}Ti_{0.8})O_3$–$0.5(Ba_{0.7}Ca_{0.3})TiO_3$ ceramic can exist in rhombohedral, orthorhombic, tetragonal, or any combination of these phases at room temperature [34]. Detailed dynamic mechanical analysis indicates that the intermediate orthorhombic phase displays an elastic storage modulus below 50 GPa [35], which is not only the lowest among all phases in this particular composition, but also much lower than that of $(Bi_{1/2}Na_{1/2})TiO_3$-based and $PbZrO_3$-based ceramics [36,37]. A very recent TEM study with convergent beam electron diffraction analysis shows that the $0.5Ba(Zr_{0.2}Ti_{0.8})O_3$–$0.5(Ba_{0.7}Ca_{0.3})TiO_3$ ceramic is a mixture of rhombohedral and tetragonal phases in its virgin state at room temperature [38]. We suggest this two-phase mixture transforms to the orthorhombic phase at moderate fields during poling, which would correspond to a significant elastic softening and the internal stresses would hence be small.

It should be pointed out that the single-domain state is not quite stable. When the poling field is removed, domain walls reappear in small portions of the grain. Even when the poling field at which the single-domain state is initially observed is maintained, domain walls start to form in regions adjacent to grain boundaries after several minutes. Figure 3 shows an example which follows the [101]-aligned grain shown in Fig. 2(d). This grain becomes a single domain immediately at the application of a poling field of 2.50 kV/cm [Fig. 2(d)]. After this field is maintained for 3 min, lamellar domains with their traces roughly along the $[1\bar{1}\bar{1}]$ direction start to nucleate from the grain boundary, as highlighted by the bright box in Fig. 3(a). Further growth of existing domains and nucleation of new domains continues as time elapses [Fig. 3(b)]. However, these domains are confined in the region close to grain boundaries and for the most part, the grain remains free of domain walls. This seems to support our elastic softening mechanism for the single-domain state. The exceptionally low elastic modulus in the poling-induced orthorhombic phase leads to low internal stresses in the polycrystalline ceramic. The weak driving force leads to delayed and slow formation of non-180° domains in small regions close to grain boundaries.

The discovery of the unique single-domain state in the $0.5Ba(Zr_{0.2}Ti_{0.8})O_3$–$0.5(Ba_{0.7}Ca_{0.3})TiO_3$ ceramic during poling has technological implications. This composition was

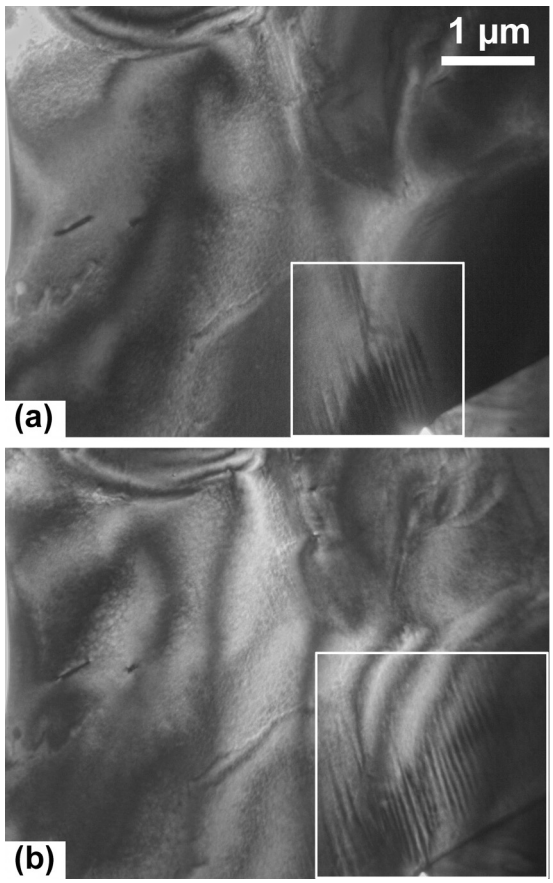

FIG. 3. The nucleation and growth of lamellar domains in the grain shown in Fig. 2(d) at 2.50 kV/cm recorded after (a) 3 min and (b) 5 min. No further domain formation was noticed in this grain beyond 5 min.

reported to display an ultrahigh piezoelectric coefficient d_{33} over 600 pC/N (Ref. [14]) and its property is highly sensitive to poling conditions [39,40]. As for a polycrystalline ferroelectric ceramic, the ultimate goal of electrical poling for piezoelectricity is to make all individual grains single domain with aligned polarizations. The observed single-domain state here is very likely the primary reason for the excellent piezoelectric property in this $BaTiO_3$-based lead-free ceramic, and its delicate nature well explains the strong dependence of d_{33} on poling conditions.

In addition to the possible well-aligned polarization, the exceptionally low elastic modulus of the single-domained orthorhombic phase may also contribute to the ultrahigh piezoelectric property of this ceramic. Generally speaking, lattice softening and low polarization anisotropy go hand in hand: both enhance the piezoelectric response [14]. Elastic softening is believed to effectively relax the crystal lattice and facilitate the structural instability when electric fields are applied. Correspondingly, high piezoelectric properties are always observed in elastically compliant phases [15,41–43],

In conclusion, the microstructural evolution during electrical poling in the $0.5Ba(Zr_{0.2}Ti_{0.8})O_3$–$0.5(Ba_{0.7}Ca_{0.3})TiO_3$ polycrystalline ceramic is investigated with *in situ* TEM. The grains of the original multidomain state transform to a unique single-domain state at very moderate poling

fields. It is suggested that this transition corresponds to the formation of a pure orthorhombic phase with a significant elastic softening. The single-domain state is suggested to be primarily responsible for the excellent piezoelectric property in this lead-free composition and its delicate nature can explain the high sensitivity of the property to poling conditions.

The National Science Foundation (NSF), through Grant No. DMR-1037898, supported this work.

[1] G. Arlt, J. Mater. Sci. **25**, 2655 (1990).
[2] D. Damjanovic, Rep. Prog. Phys. **61**, 1267 (1998).
[3] S. Nambu and D. A. Sagala, Phys. Rev. B. **50**, 5838 (1994).
[4] P. Ondrejkovic, P. Marton, M. Guennou, N. Setter, and J. Hlinka, Phys. Rev. B **88**, 024114 (2013).
[5] J. Sapriel, Phys. Rev. B **12**, 5128 (1975).
[6] T. Sluka, A. K. Tagantsev, D. Damjanovic, M. Gureev, and N. Setter, Nat. Commun. **3**, 748 (2012).
[7] B. Jaffe, W. R. Cook, and H. Jaffe, *Piezoelectric Ceramics* (Academic, London 1971).
[8] L. X. Zhang and X. Ren, Phys. Rev. B **71**, 174108 (2005).
[9] Z. H. Zhang, X. Y. Qi, and X. F. Duan, Appl. Phys. Lett. **89**, 242905 (2006).
[10] P. Zheng, J. L. Zhang, Y. Q. Tan, and C. L. Wang, Acta Mater. **60**, 5022 (2012).
[11] Y. Qin, J. Zhang, Y. Gao, Y. Tan, and C. Wang, J. Appl. Phys. **113**, 204107 (2013).
[12] K. L. Kim, N. T. Tsou, and J. E. Huber, J. Appl. Phys. **113**, 194104 (2013).
[13] C. Ma, H. Z. Guo, S. P. Beckman, and X. Tan, Phys. Rev. Lett. **109**, 107602 (2012).
[14] W. Liu and X. Ren, Phys. Rev. Lett. **103**, 257602 (2009).
[15] D. Xue, Y. Zhou, H. Bao, C. Zhou, J. Gao, and X. Ren, J. Appl. Phys. **109**, 054110 (2011).
[16] H. Z. Guo, S. Zhang, S. P. Beckman, and X. Tan, J. Appl. Phys. **114**, 154102 (2013).
[17] X. Tan, H. He, and J. K. Shang, J. Mater. Res. **20**, 1641 (2005).
[18] H. Z. Guo, C. Ma, X. M. Liu, and X. Tan, Appl. Phys. Lett. **102**, 092902 (2013).
[19] X. Tan, Z. Xu, J. K. Shang, and P. Han, Appl. Phys. Lett. **77**, 1529 (2000).
[20] J. Gao, D. Xue, Y. Wang, D. Wang, L. Zhang, H. Wu, S. Guo, H. Bao, C. Zhou, W. Liu, S. Hou, G. Xiao, and X. Ren, Appl. Phys. Lett. **99**, 092901 (2011).
[21] M. L. Mulvihill, L. E. Cross, W. Cao, and K. Uchino, J. Am. Ceram. Soc. **80**, 1462 (1997).
[22] L. X. Zhang and X. Ren, Phys. Rev. B **73**, 094121 (2006).
[23] J. Wu, D. Xiao, W. Wu, Q. Chen, J. Zhu, Z. Yang, and J. Wang, J. Eur. Ceram. Soc. **32**, 891 (2012).
[24] J. Hirohashi, K. Yamada, H. Kamio, M. Uchida, and S. Shichijyo, J. Appl. Phys. **98**, 034107 (2005).
[25] C. Ma and X. Tan, Solid State Commun. **150**, 1497 (2010).
[26] C. A. Randall, D. J. Barber, and R. W. Whatmore, J. Microsco.-Oxford **145**, 275 (1987).
[27] V. A. Isupov, Ferroelectrics **315**, 123 (2005).
[28] S. B. Vakhrushev, V. A. Isupov, B. E. Kvyatkovsky, N. M. Okuneva, I. P. Pronin, G. A. Smolensky, P. P. Syrnikov, and A. F. Ioffe, Ferroelectrics **63**, 153 (1985).
[29] W. Ge, J. Yao, L. Luo, C. P. Devreugd, J. Li, and D. Viehland, J. Am. Ceram. Soc. **94**, 478 (2011).
[30] W. Qu, X. Zhao, and X. Tan, J. Appl. Phys. **102**, 084101 (2007).
[31] R. E. Newnham, *Properties of Materials: Anisotropy, Symmetry, Structure* (Oxford University Press, New York, 2005).
[32] P. Yang, and D. A. Payne, J. Appl. Phys. **80**, 4001 (1996).
[33] X. Tan, C. Ma, J. Frederick, S. Beckman, and K. G. Webber, J. Am. Ceram. Soc. **94**, 4091 (2011).
[34] D. S. Keeble, F. Benabdallah, P. A. Thomas, M. Maglione, and J. Kreisel, Appl. Phys. Lett. **102**, 092903 (2013).
[35] D. Damjanovic, A. Biancoli, L. Batooli, A. Vahabzadeh, and J. Trodahl, Appl. Phys. Lett. **100**, 192907 (2012).
[36] Y. Yao, Z. Sun, Y. Ji, Y. Yang, X. Tan, and X. Ren, Sci. Technol. Adv. Mater. **14**, 035008 (2013).
[37] S. E. Young, H. Z. Guo, C. Ma, M. R. Kessler, and X. Tan, J. Therm. Anal. Calorim. **115**, 587 (2014).
[38] J. Gao, L. Zhang, D. Xue, T. Kimoto, M. Song, L. Zhong, and X. Ren, J. Appl. Phys. **115**, 054108 (2014).
[39] M. C. Ehmke, S. N. Ehrlich, J. E. Blendell, and K. J. Bowman, J. Appl. Phys. **111**, 124110 (2012).
[40] M. C. Ehmke, J. Daniels, J. Glaum, M. Hoffman, J. E. Blendell, and K. J. Bowman, J. Am. Ceram. Soc., doi:10.1111/jace.12586 (2013).
[41] S. J. Zhang and F. Li, J. Appl. Phys. **111**, 031301 (2012).
[42] A. K. Singh, S. K. Mishra, Ragini, D. Pandey, S. Yoon, S. Baik, and N. Shin, Appl. Phys. Lett. **92**, 022910 (2008).
[43] F. Tasnádi, B. Alling, C. Höglund, G. Wingqvist, J. Birch, L. Hultman, and I. A. Abrikosov, Phys. Rev. Lett. **104**, 137601 (2010).